Raytheon
Customer Success Is Our Mission

Vicarious calibration of moderate resolution sensors using the specular array radiometric calibration (SPARC) method

Raytheon Space and Airborne Systems
Stephen J. Schiller
Jeffery J. Puschell

CEOS WGCV IVOS workshops and meetings
13-17 March, 2017
College of Optical Sciences
University of Arizona

Introduction

- Vicarious calibration has played an important role in the in-flight radiometric assessment of Earth observing sensor systems for many years, principally to validate the absolute performance of the on-board calibrator.
- The effort moving into the future considers the potential to move vicarious methods into a more prominent calibration role potentially replacing on-board absolute calibration. The objective is to reduce cost and schedule through lower power, weight, and volume in future designs.
- This presentation describes a on-going effort to support this objective using Raytheon's Specular Array Radiometric Calibration (SPARC) method in a vicarious calibration study of Landsat 8 and Sentinal-2.
- NASA support for this research is gratefully acknowledged through the NASA ROSES program grant No. NNX15AV43G.

Conceptualizing The SPARC Method

The SPARC method allows any earth observing sensor to image the sun, just like a solar radiometer, and be calibrated directly to the solar spectral constant The reflective Field-of-Regard for a mirror acts as a Field-of-View (FOV) aperture stop just as with an aperture stop on a typical sun photometer allowing the sun to be viewed directly as an absolute reference.

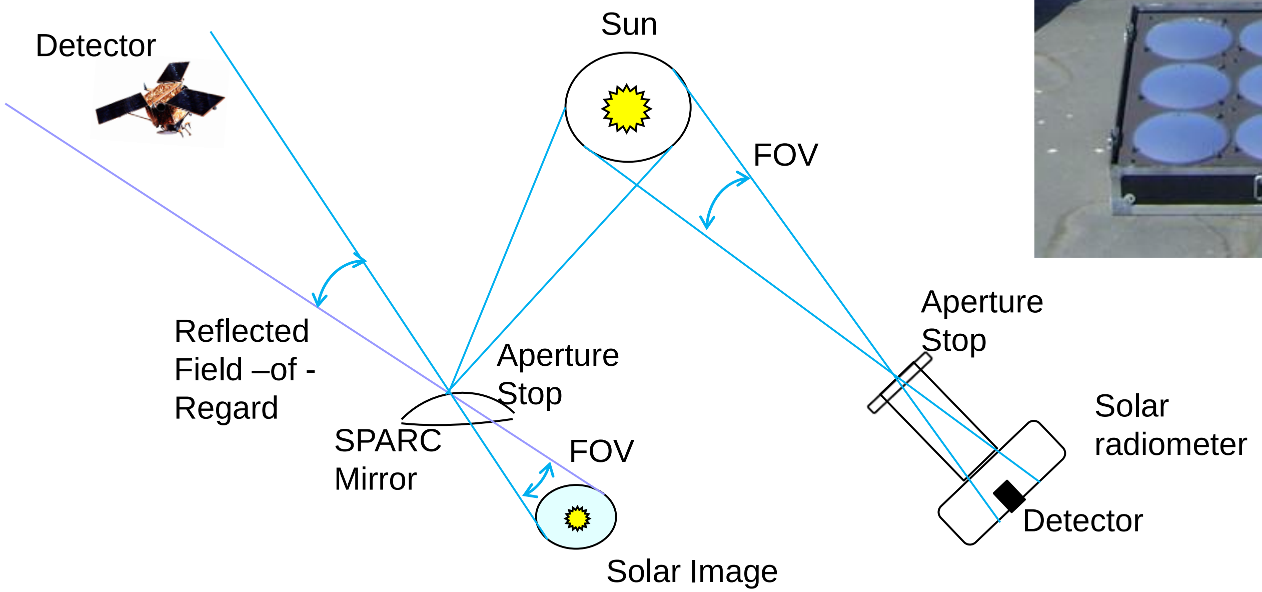

The mirror also acts as an ideal neutral density filter. By selecting an appropriate radius of curvature of the mirror, it scales down the brightness of the sun to an intensity that does not saturate the sensor focal plane and does so without changing upwelling spectral properties.

SPARC Method Applied to the Absolute Calibration of High Spatial Resolution Sensors

- Site: Parking lot of Raytheon SAS Facility in El Segundo, CA. Two miles south of the

- Site: Natural grass field located at Clairmont, CA

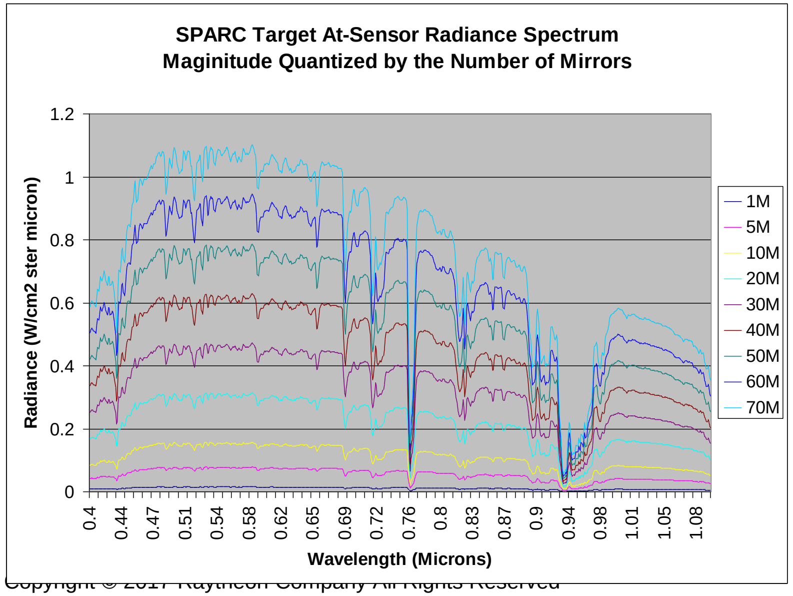

SPARC Radiometric Calibration Capability Heritage

- Method has been demonstrated with IKONOS and Quickbird

IKONOS

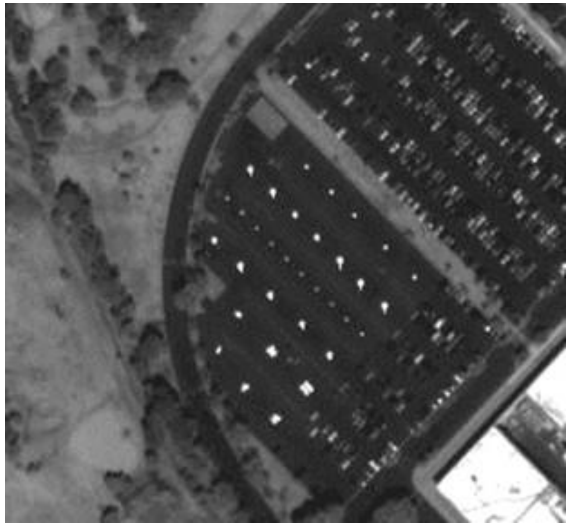

The SPARC method has been applied to small footprint sensors demonstrating its capability of providing accurate and repeatable radiometric references for calibration applications

Quickbird

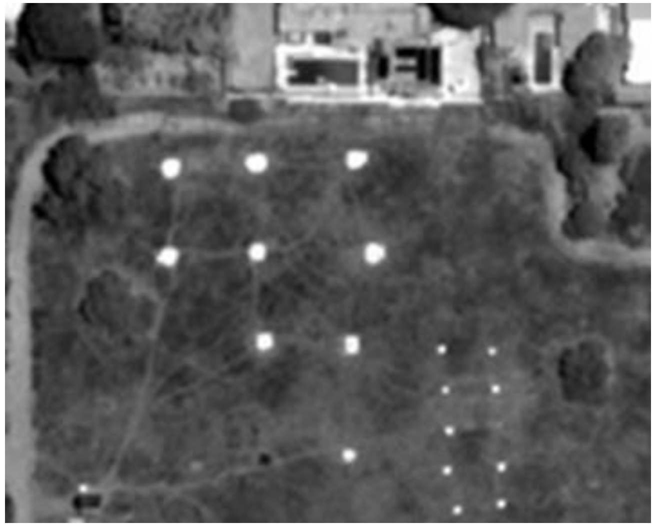

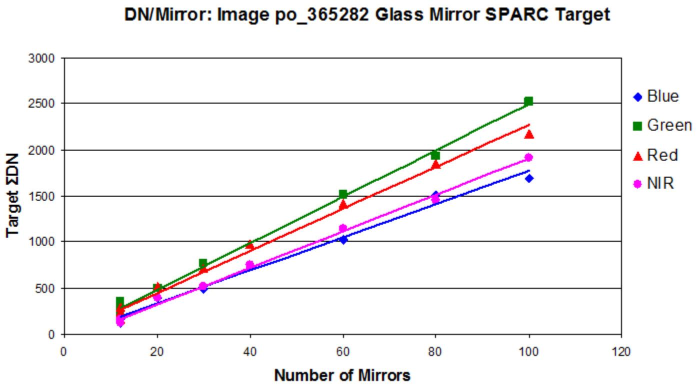

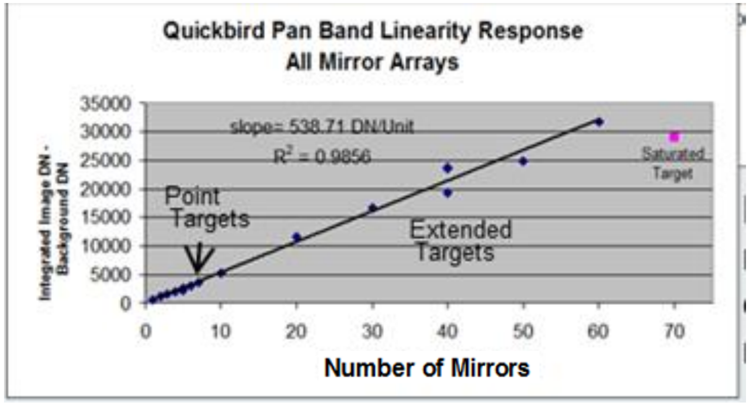

Plots demonstrate consistency in the radiometric response to SPARC targets over the sensor dynamic range.

Raytheon

SPARC Absolute Radiative Transfer Equation

- The absolute radiometric calibration of a sensor proceeds from the SPARC radiative transfer equation.

At-Sensor In Band Radiance/mirror For A SPARC Target

$$L_{at-sensor}(\lambda)/mirror = \rho(\lambda)\tau_{\downarrow}(\lambda)\tau_{\uparrow}(\lambda)E_o(\lambda)\left(\frac{R}{2GSD}\right)^2$$

Watts/(m^2 sr micron)

$\rho\ (\lambda,\theta_r)$ = Mirror specular reflectance
$\tau_{\downarrow}\ (\lambda)$ = Sun to ground transmittance
$\tau_{\uparrow}\ (\lambda)$ = Ground to sensor transmittance

$E_o\ (\lambda)$ = Solar spectral constant
R = Mirror radius of curvature (m)
GSD = Ground sample distance normal to line-of-sight (m)

- The radiance is the total integrated energy reaching the sensor within a SPARC target image profile
- The goal is to compare the vicarious SPARC predicted radiance to the sensor radiance reported in the Landsat 8 L1R calibrated imagery for individual targets

Raytheon

SPARC Target Design For Landsat 8

Because SPARC targets are specular intensity sources and Landsat has a large GSD, the mirror radius of curvature is much larger than used with commercial sensors to produce the same effective radiance.

The reflected field-of-regard produces a uniform illumination intensity across the sky
= 4.5 degrees

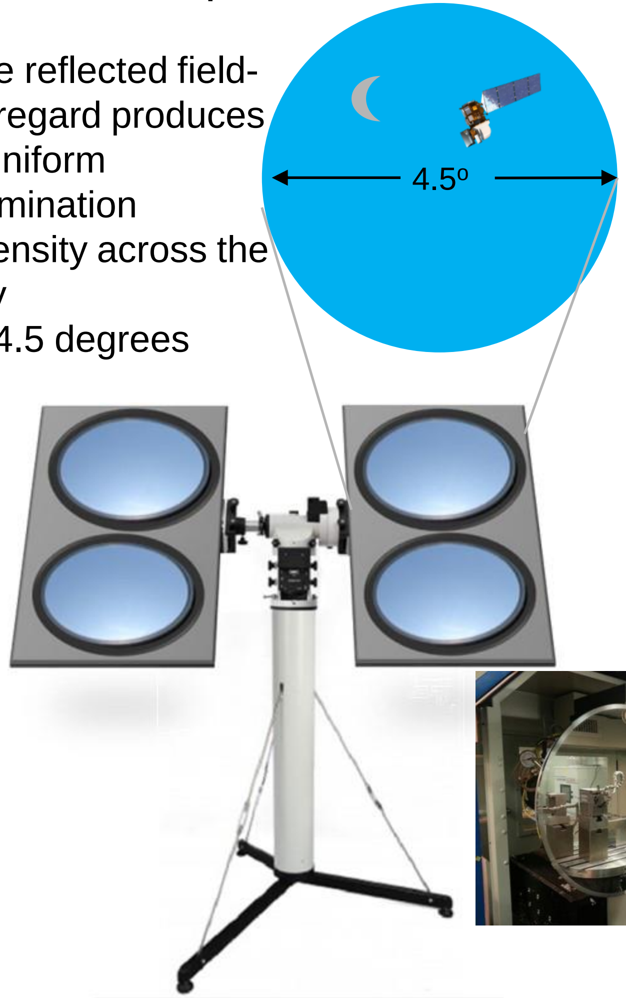

SPARC Calibration Panels:

- Four 18” diameter mirrors on each telescope mount (9 lbs each)
- 10 m Radius of curvature mirrors
- Clear Field-of-Regard (FOR) = 4.5º
- Deployed on a portable iOptron® iEQ45 ProTM alt-az telescope mount.
- Built-in 32-channel Global Positioning System (GPS).
- Payload mirror assembly on each mount is about 50 lbs
- Four deployable panels (each on separate mounts) are used to provide up to 3 calibration radiance levels in a single Landsat image collect.

SPARC Radiometric Target Designed For Landsat 30 m Multispectral Calibration

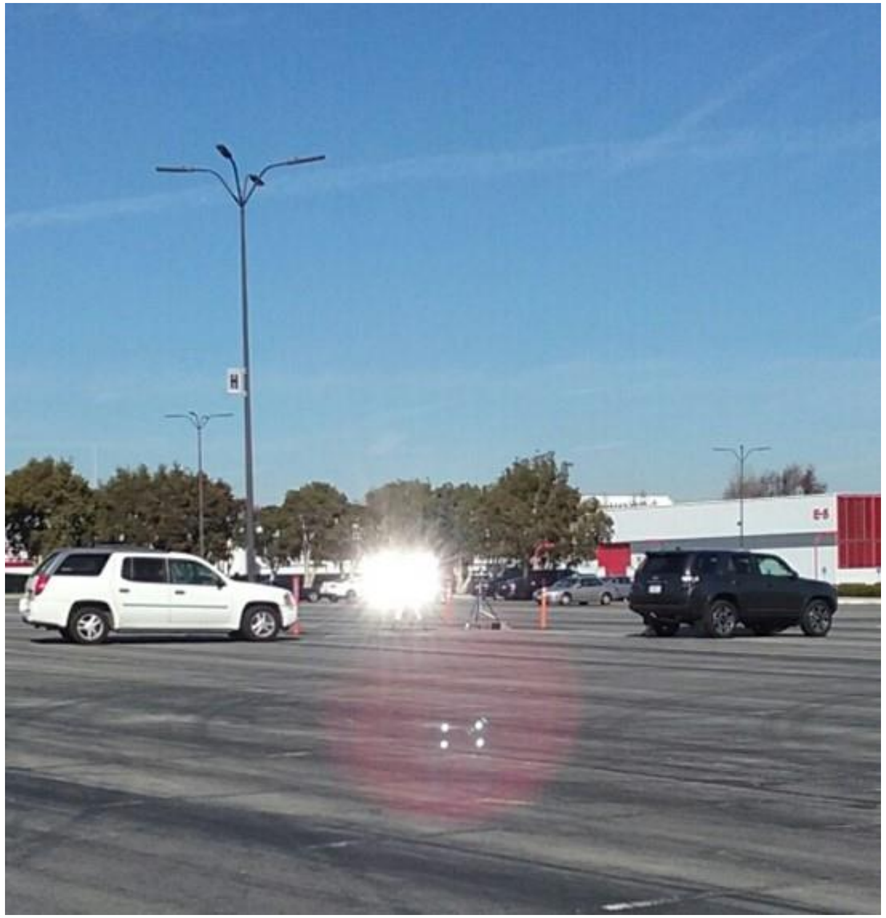

Portable system provides computer controlled pointing with sub-arcminute resolution and potential satellite tracking capability

L8 Pan Image SPARC target Response

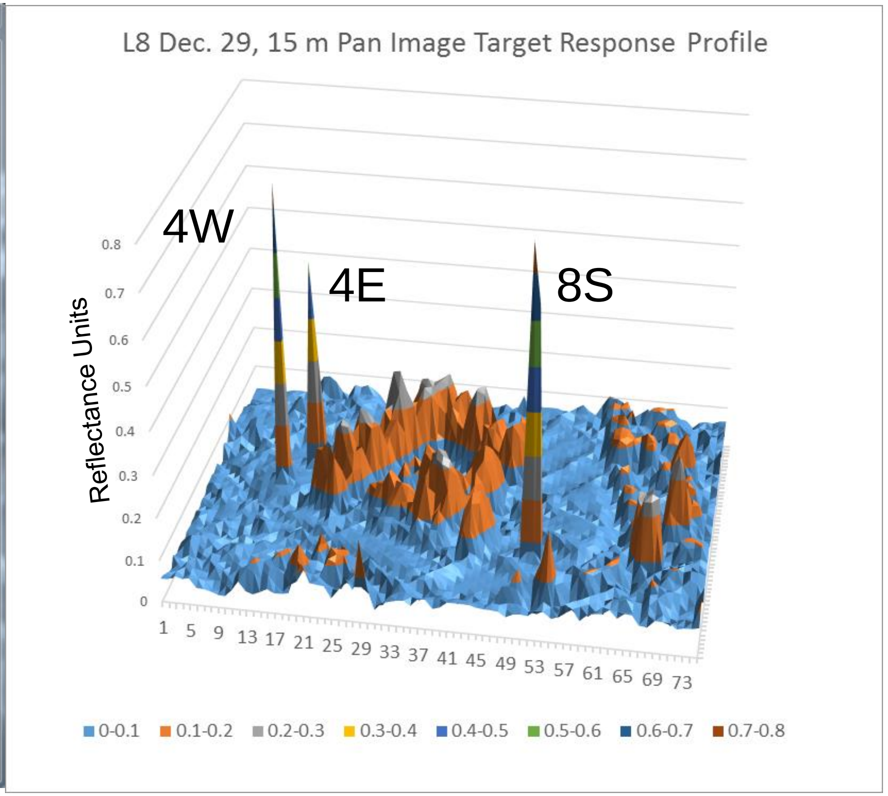

3D plot shows the relative brightness of the mirror targets compared to the rest of the scene. The central pixel response to target 8S is equivalent to a top-of-atmosphere Lambertian diffuse reflector of about 80% reflectance.

Dec. 29 L8 Green Multispectral Band

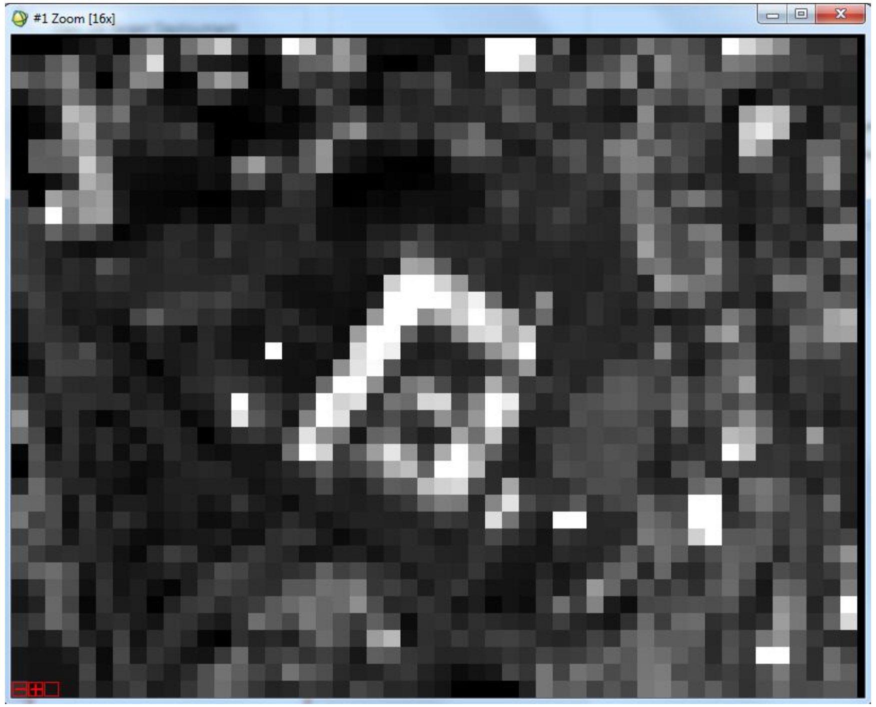

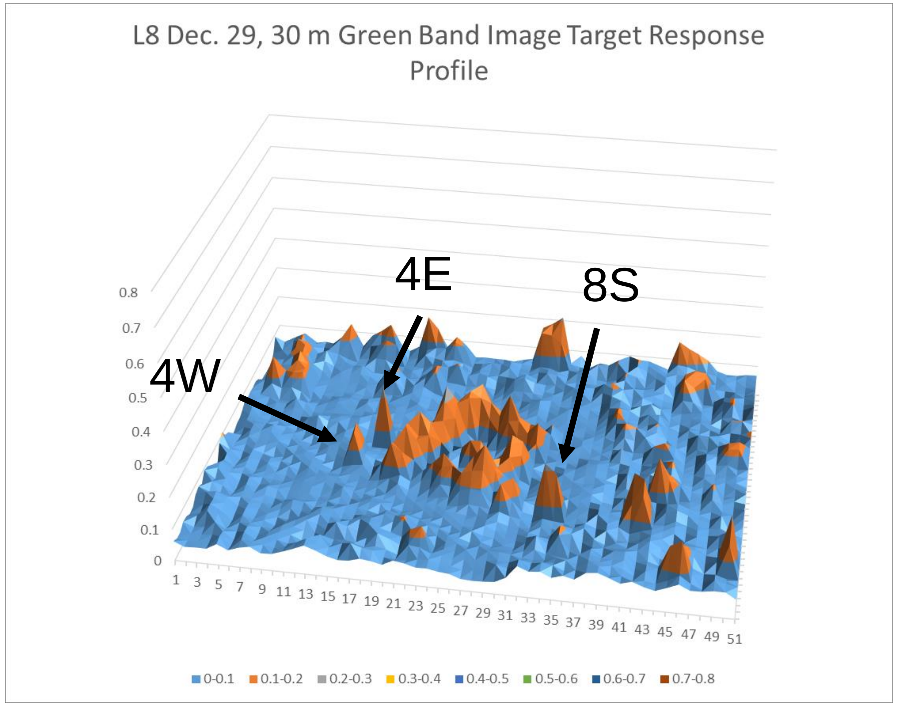

Acting as point targets, the multispectral bands response is much less than the Pan Band. Doubling the GSD from 15 m to 30 m decreases the integrated response by a factor of 4. The result is a response for the S8 target equivalent to a 20% Lambertian diffuser

SPARC Target Images For Oversampling PSF

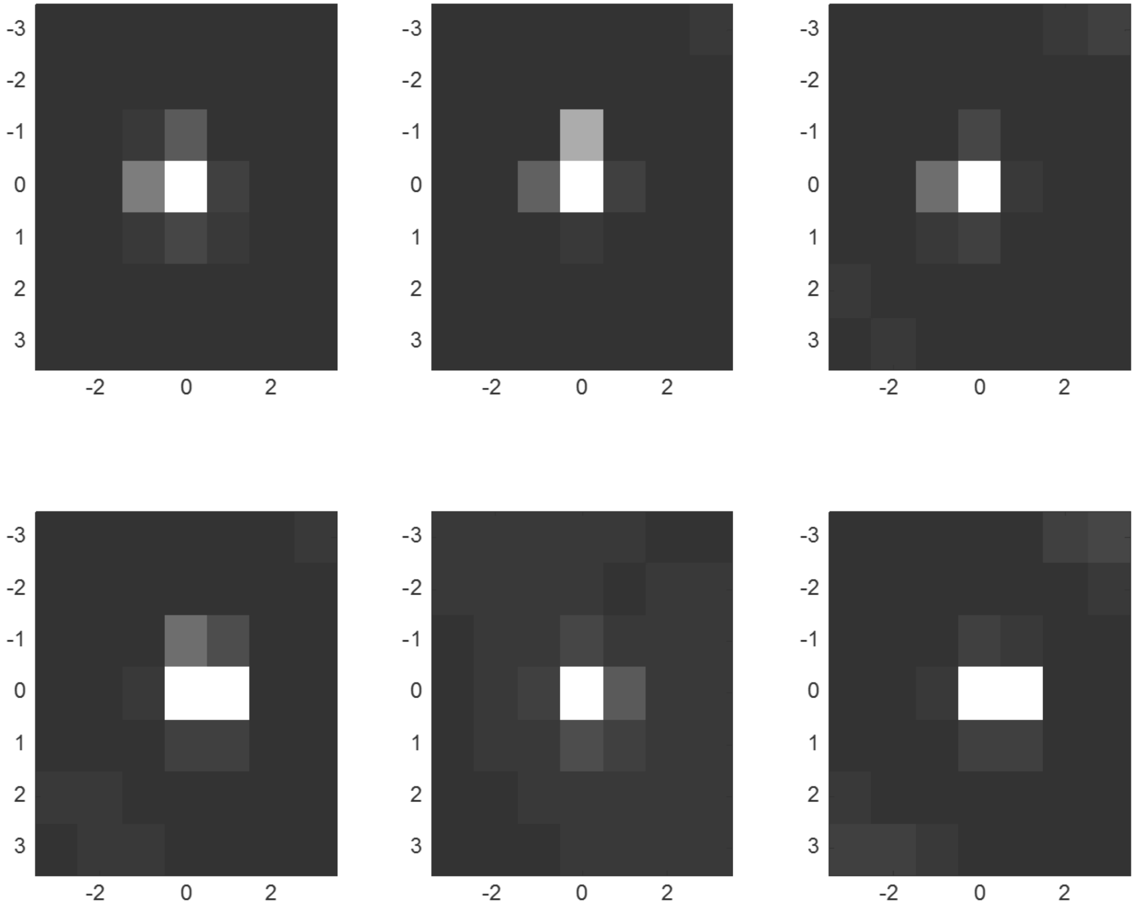

Each 7 x7 pixel image (15 m GSD) is fit with a Gaussian profile using regression analysis to locate individual centroids and align to a common center to produce the composite oversampled 2D PSF profile.

Sensor System Composite 2D PSF Profile For L8 Pan Band

Cross-scan and along-scan slices through the composite profile center

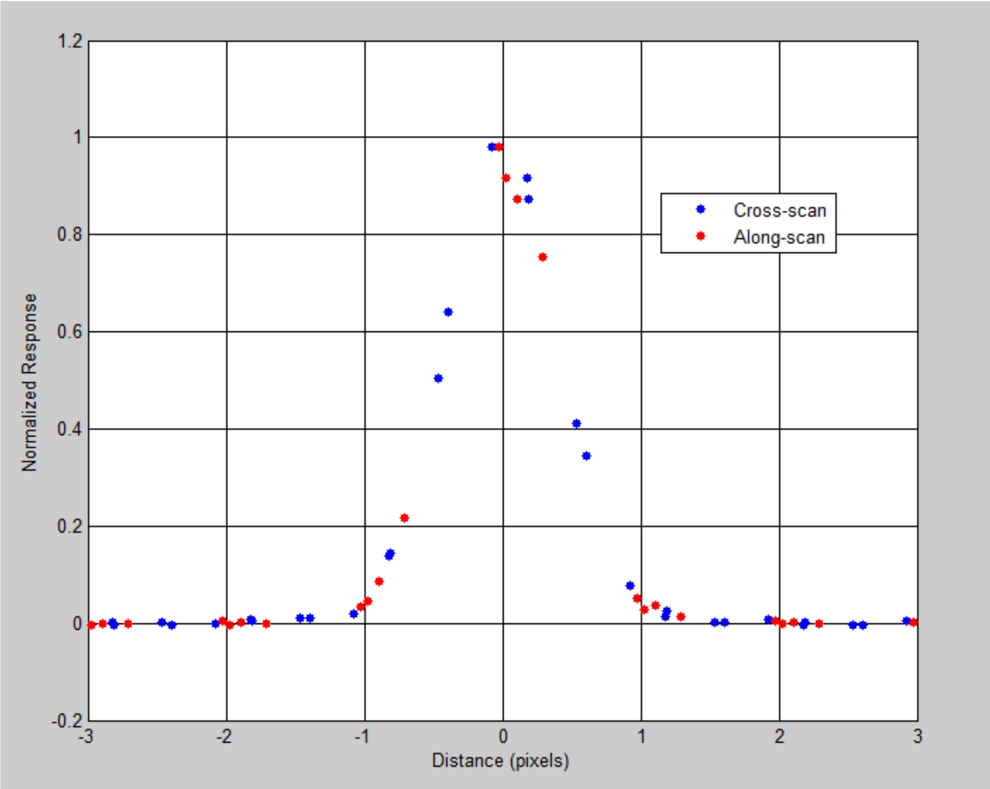

Composite 2D PSF Profile Residuals show no outliers

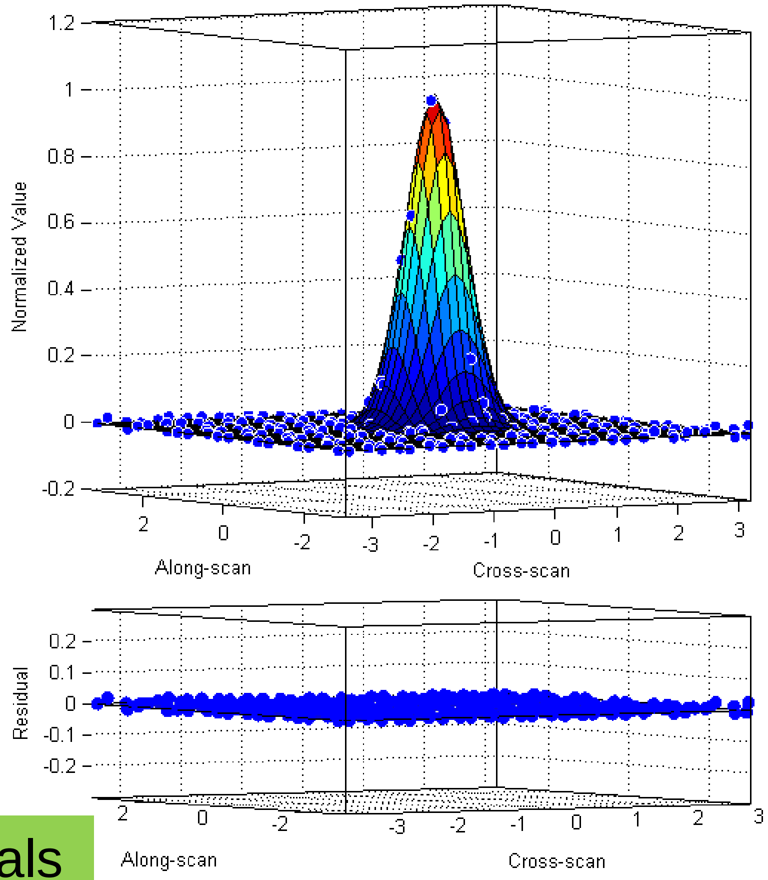

System level PSF shows negligible residuals when modeled as a Gaussian function.

SPARC Target Data

- Both L1R and L1T products were obtained from this overpass.

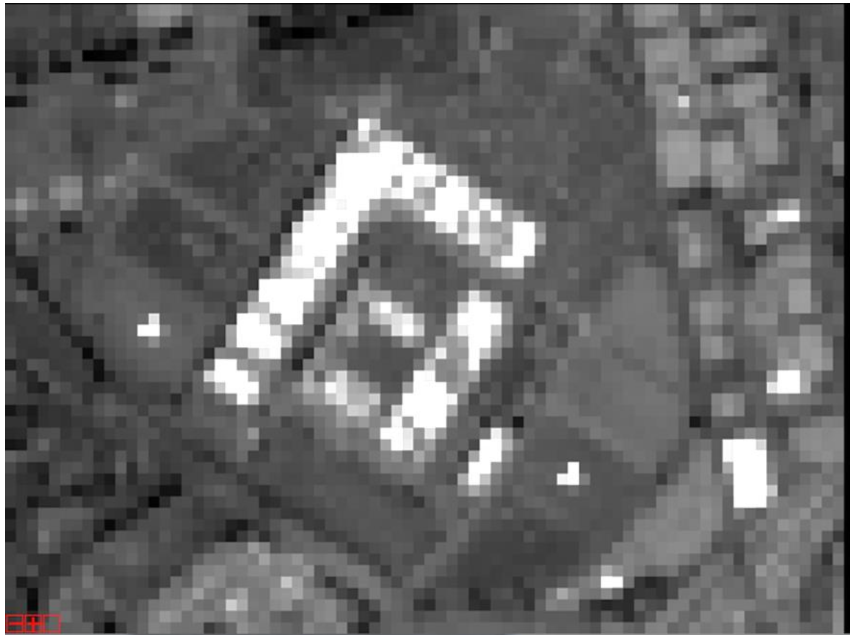

L1R Pan Image

L1T Pan Image

The change in the spatial appearance of each SPARC target between the L1R and L1T product from the cubic convolution resampling is easily seen.

To assess the effects of resampling on small target radiometry, the same integrated radiance measurement process of these two targets will be applied to both images

Sensor System Composite 2D PSF Profile For L8 Pan Band

Composite L1R product 2D PSF profile residuals show no outliers

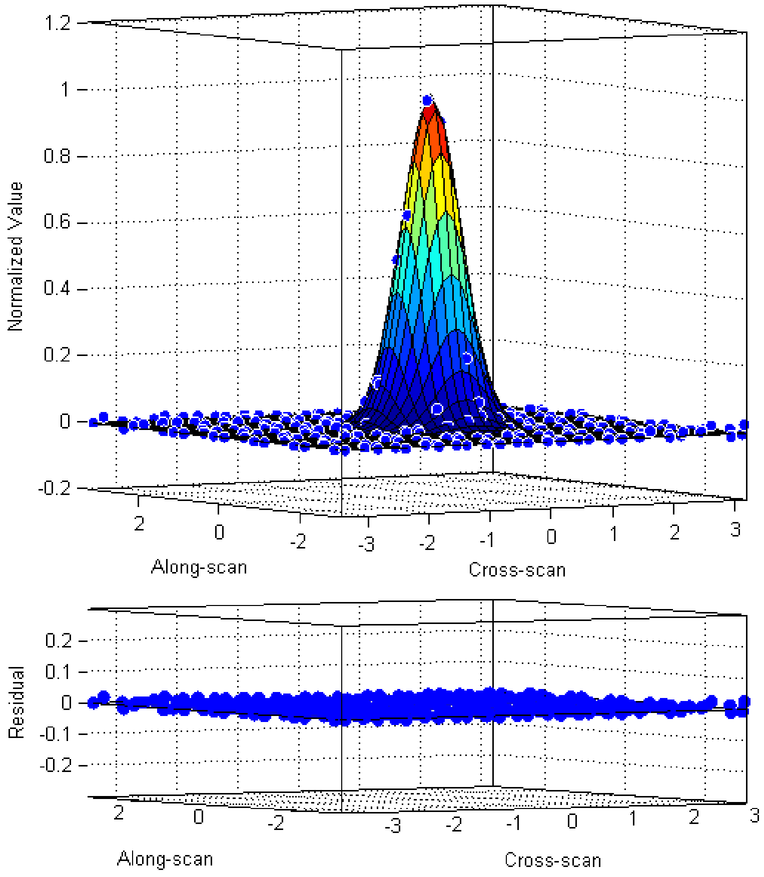

Composite L1T product 2D PSF profile reveals significant degradation in the average system PSF from the resampling process.

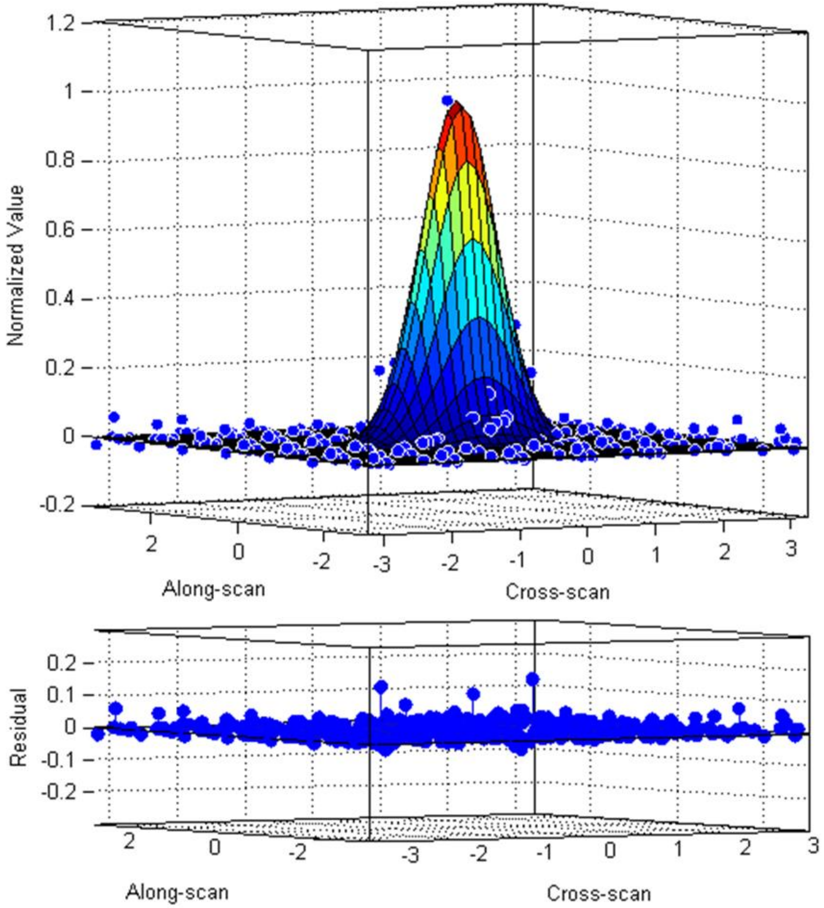

Cross-scan and along-scan slices through the composite profile center

Raytheon

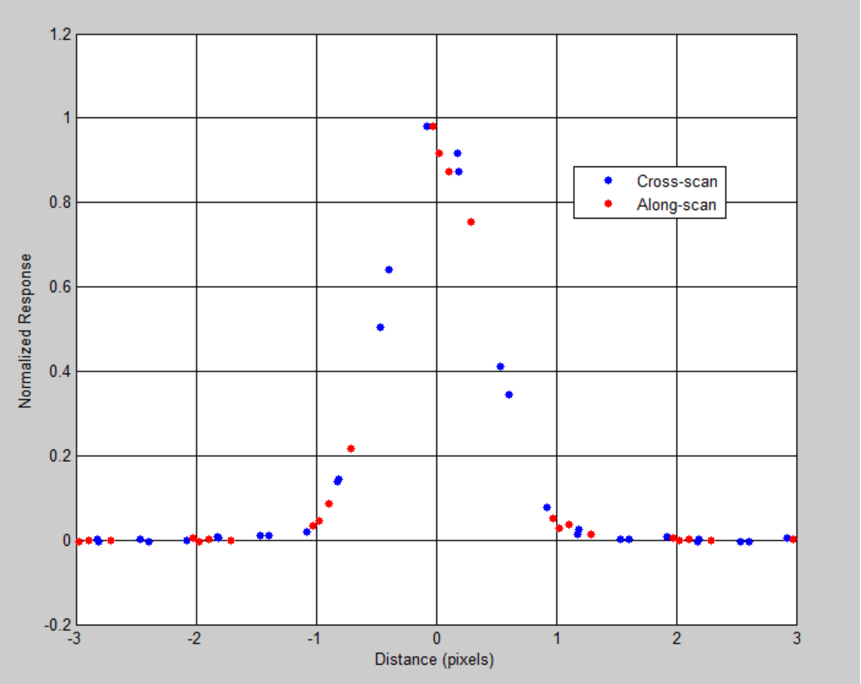

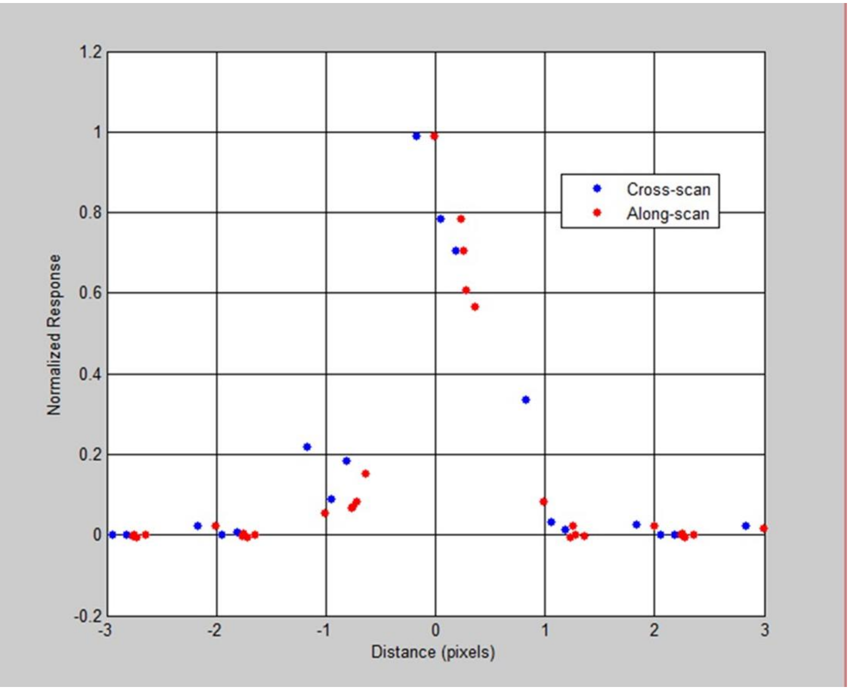

The well characterized PSF profile revealed in the L1R data shows significant degradation in the L1T data due to resampling.

L1R Profile

L1T Profile

L1R PSF	PSF FWHM (Pixels, 15 m)	Goodness if Fit R^2	MTF @ Nyquist	Relative Edge Response
Cross-Scan	0.977 ± 0.003	0.9978	0.4275	0.7718
Along-Scan	0.959 ± 0.005	0.9978	0.4411	0.7840

Feb. 15, 2016 Target Deployment

- Two identical mirror targets were set up 400 m apart in the El Segundo Parking lot (labeled 8N and 8S)
- Each target consisted of two aligned panels containing a total of 8 mirrors

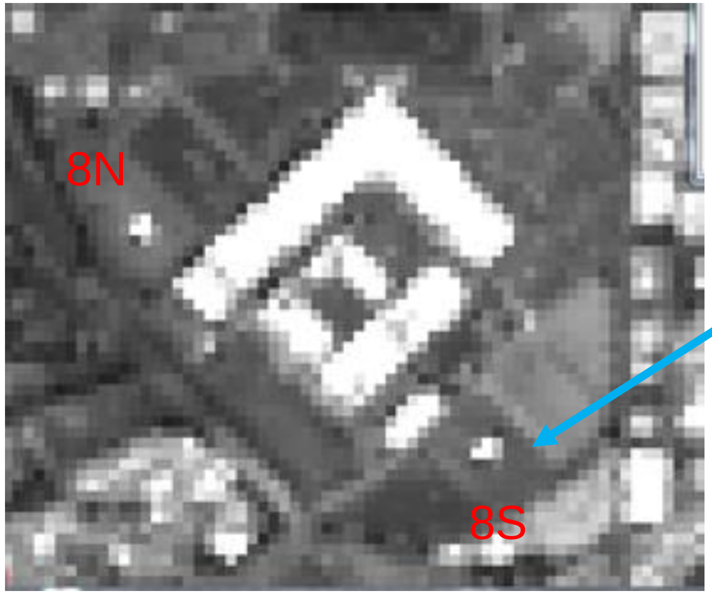

- The Feb. 15 pan image above shows the location of the two targets

Integrated Radiance Measurements

- The following images show the ROI placement used to calculate the integrated radiance form the L8 green band image.
- For each 2x2 pixel target area, the subpixel centroid was located and the pixel phasing offset applied to improve the ensquared energy correction estimate.

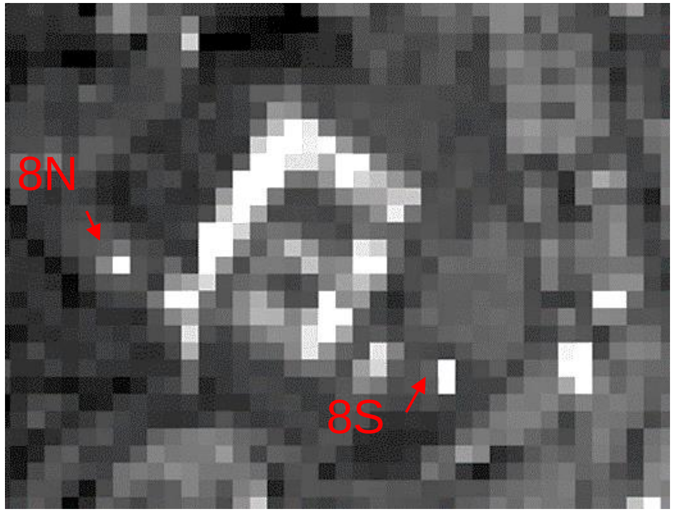

North

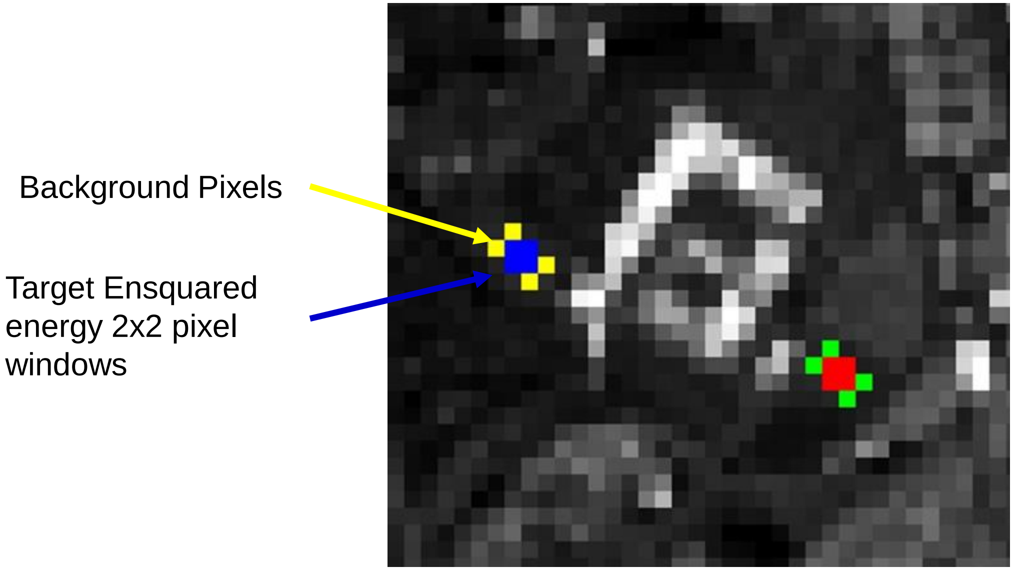

Target Radiometric Repeatability
For The Feb. 15 8N and 8S SPARC Reference Sources

- The following table and plot compares the L8 measured relative radiance between two equivalent SPARC targets, [% Diff (8S-8N)/(0.5*(8S+8N)],
- The maximum 1σ uncertainty difference is estimated to be ~ 5.4% (orange 1σ error bar)

L8 Spectral Band	CA	Blue	Green	Red	NIR	SWIR1	SWIR2	Pan
Band Center (nm)	442.90	482.00	561.40	654.60	864.70	1608.90	2200.70	589.50
8S Measured From Image (W/m^2 sr um)	225.12	255.10	279.66	266.22	153.67	44.37	14.84	268.81
8N Measured from Image (W/m^2 sr um)	214.86	252.03	270.40	260.15	176.83	43.41	13.87	251.63
% Diff (8S - 8N)/(0.5*(8S+8N))	**4.78%**	**1.22%**	**3.43%**	**2.33%**	**-13.09%**	**2.21%**	**6.99%**	**6.82%**

Except for the NIR band, all channels measure a difference expected within the estimated uncertainty

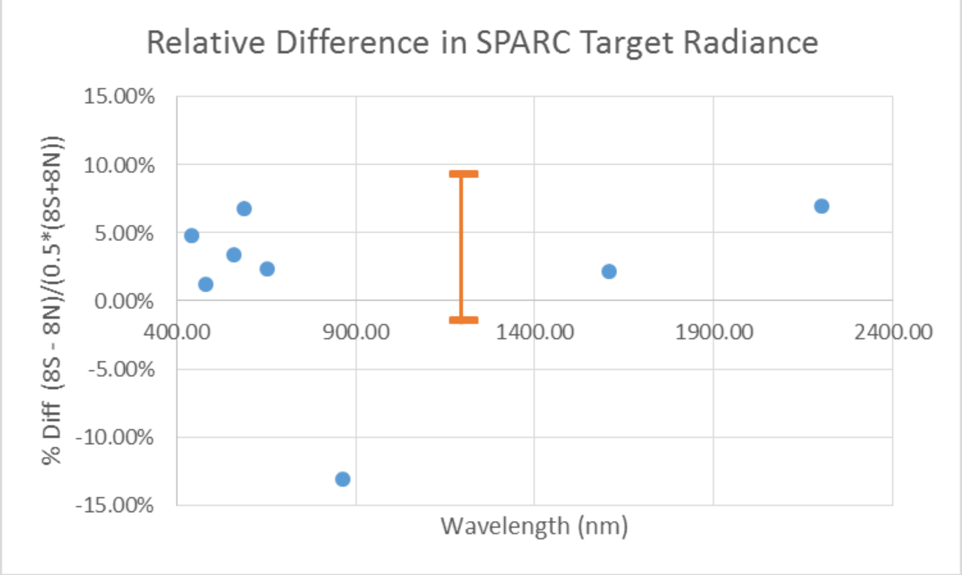

The NIR outlier appears to be a non-uniform energy-on-detector response issue for the detectors containing the target image centroid

Mirror Reflectance Measurements

Mirror witness samples were measured in the Raytheon Optical Materials Measurements Laboratory with a Perkin Elmer reflectometer.

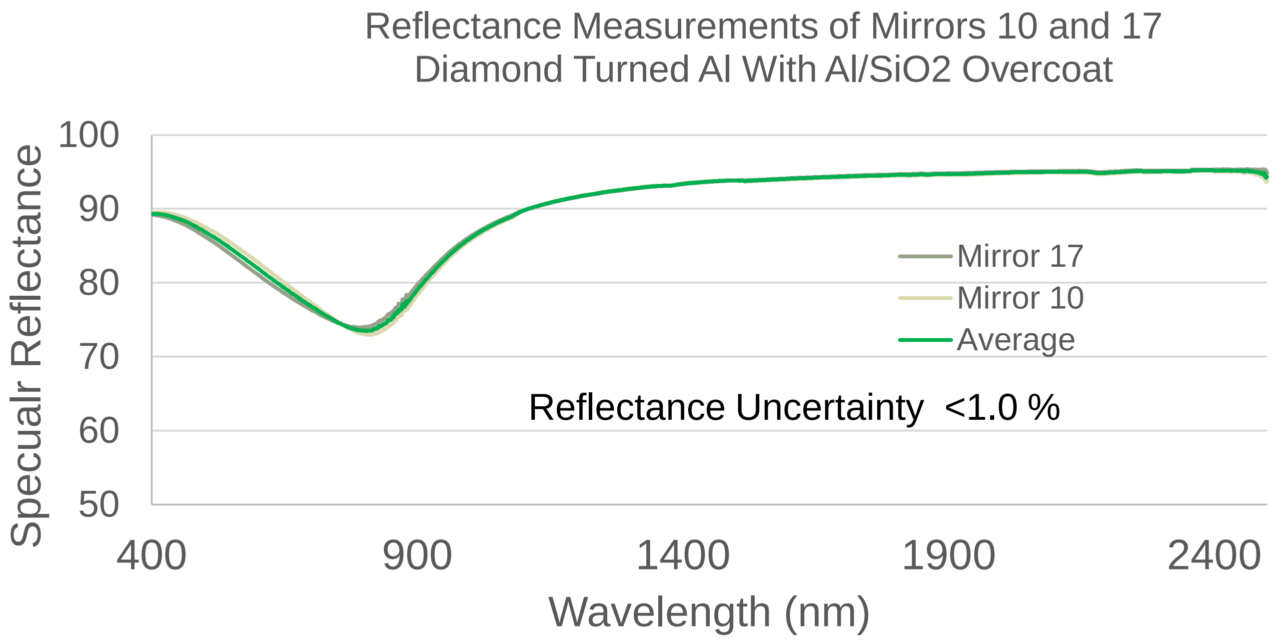

	Band Integrated Reflectance							
	CA	Blue	Green	Red	NIR	SWIR1	SWIR2	Pan
Band Center (nm)	442.9	482	561.4	654.6	864.7	1608.9	2200.7	589.5
Reflectance	88.82	87.56	83.96	79.04	76.16	94.08	94.99	82.33

Seven Band Shadow Band Radiometer for Measuring Atmospheric Transmittance

The atmospheric transmittance at each overpass is measured using a seven channel shadowband radiometer. Measurement is every 15 seconds, averaged to 1 minute intervals.

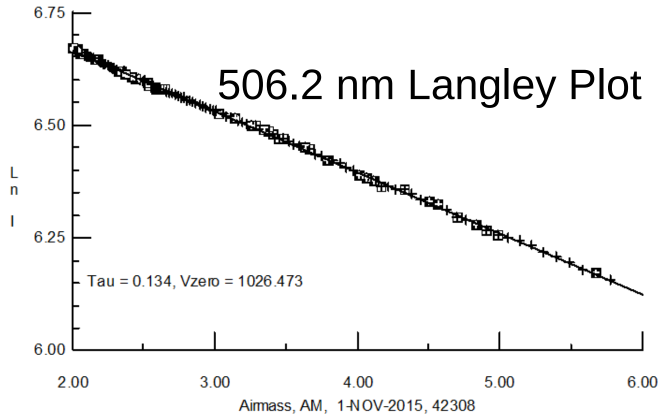

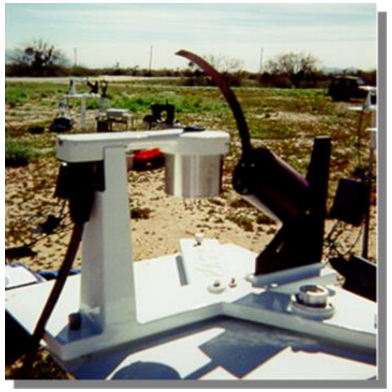

Calibrated using the Langley plot method from data collected at Table Mountain Observatory (7500 ft) over 5 weeks in Oct. and Nov. 2015

Top-of-atmosphere irradiance calibration coefficients based on 28 morning and afternoon Langley plots

Wavelength (nm)	413.9	506.2	616.8	675.5	868.5
I_o Average (1 AU)	1370.708	996.7491	305.9666	543.4447	1885.081
Std Dev.	14.403	11.415	7.111	6.199	14.163
%Error	1.051	1.145	2.324	1.141	0.751

Sky conditions On Feb. 15 Were Nearly Ideal At Overpass

- Minimal aerosol loading indicated by a best fit at a Visibility setting of VIS = 210 km and relative humidity at only 25%.
- Temperature was 85ºF and no surface wind

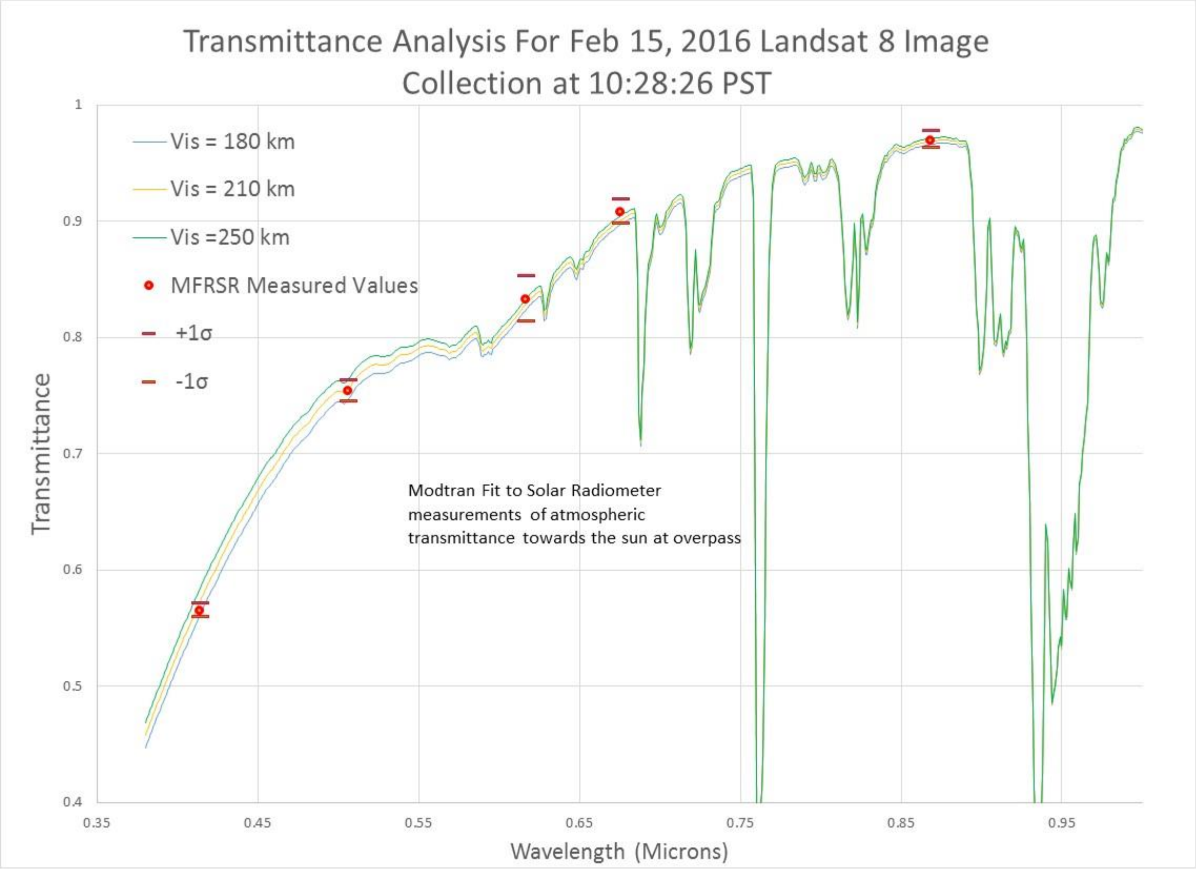

MODTRAN Model Spectrum Is Integrated With Band Spectral Response To Determine In-band Transmittance

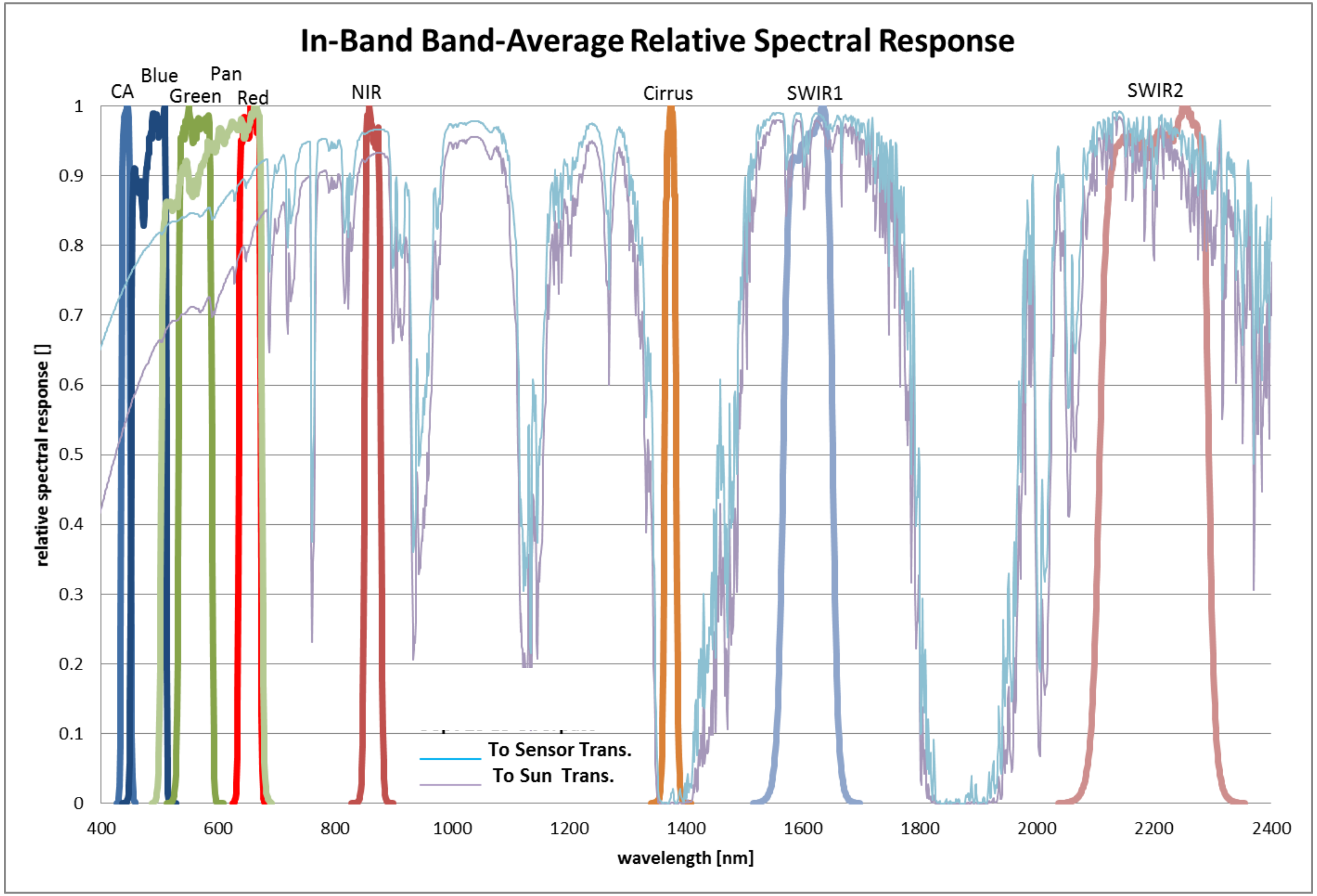

Calculation Of Vicarious Predicted At-Sensor Radiance Of SPARC Targets For the Feb. 15 Overpass

$$L_{at-sensor}(\lambda)/mirror = \rho(\lambda)\tau_{\downarrow}(\lambda)\tau_{\uparrow}(\lambda)E_o(\lambda)\left(\frac{R}{2GSD}\right)^2$$

$E_o(\lambda)$= Modtran CHKUR In-band TOA Solar Irradiance
R = 10 m and GSD = 28.8 m (measured from L1R image product)

L8 Band	CA	Blue	Green	Red	NIR	SWIR1	SWIR2	Pan
Band Center (nm)	442.9	482	561.4	654.6	864.7	1608.9	2200.7	589.5
Reflectance	0.8882	0.8756	0.8396	0.7904	0.7616	0.9408	0.9499	0.8233
To Sun Trans	0.6512	0.7265	0.7907	0.8739	0.9668	0.9646	0.9413	0.8160
To Sensor Trans	0.7685	0.8218	0.8656	0.9204	0.9795	0.9766	0.9618	0.8823
Eo (W/m2 um)	1888	1975	1852	1570	951.2	242.4	82.49	1751
Radiance /mirror (W/m2*str*um)	25.30	31.12	32.08	30.09	20.68	6.48	2.14	31.28
8 mirrors (W/m2*str*um)	202.37	248.95	256.63	240.68	165.43	51.80	17.11	250.25

Absolute Radiance Comparison Between SPARC Predicted and L8 Measured Radiance

Raytheon

- The following table presents the difference between the L8 measured radiance and the SPARC vicarious predicted radiance, [%Diff (vicarous-L8)/L8], for the Feb 15 collect.
- Based on the estimated uncertainties in the two quantities, the 1σ difference should be ~ 5.0%

L8 Spectral Band	CA	Blue	Green	Red	NIR	SWIR1	SWIR2	Pan
Band Center (nm)	442.90	482.00	561.40	654.60	864.70	1608.90	2200.70	589.50
Predicted SPARC Radiance (Vicarious)	202.37	248.95	256.63	240.68	165.43	51.80	17.11	250.25
Mean 8N and 8S L8 measured Radiance (L8)	219.99	253.56	275.03	263.19	165.23	43.89	14.35	260.22
%Diff (vicarous-L8)/L8	**-8.01%**	**-1.82%**	**-6.69%**	**-8.55%**	**0.12%**	**18.02%**	**19.17%**	**-3.83%**

Raytheon

Radiance Analysis Results for Feb 15, 2016 Collect

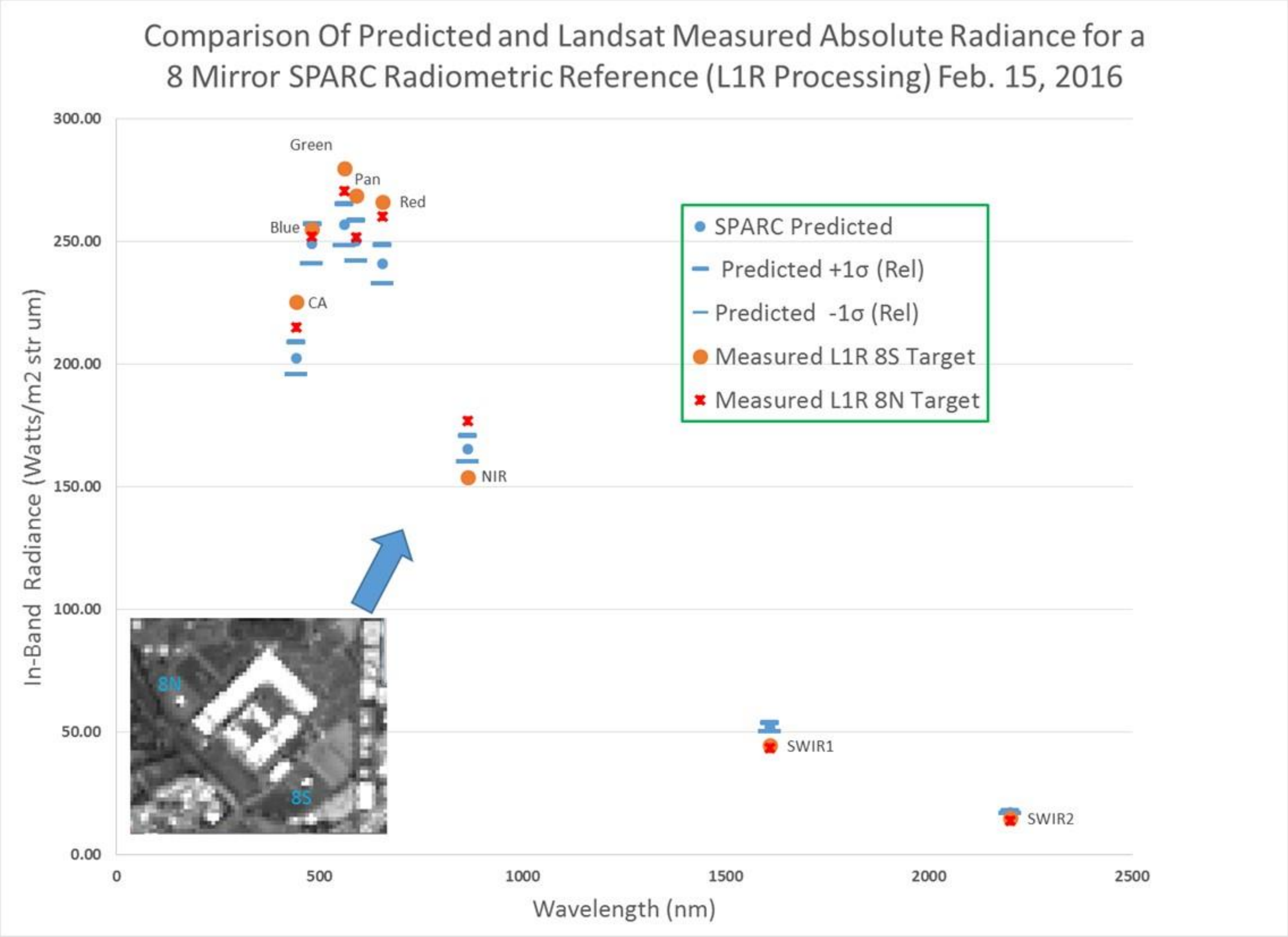

4/3/2017

Sentinel 2A 10 m GSD Image Presentation of SPARC Targets

- Targets are subpixel, > 1.5 m in size.
- The intensity step size is incremental from 1 to 4 without saturation.
- Targets are visibly affecting pixels in a 6 x 6 pixel area (processing includes resampling for orthorectification).

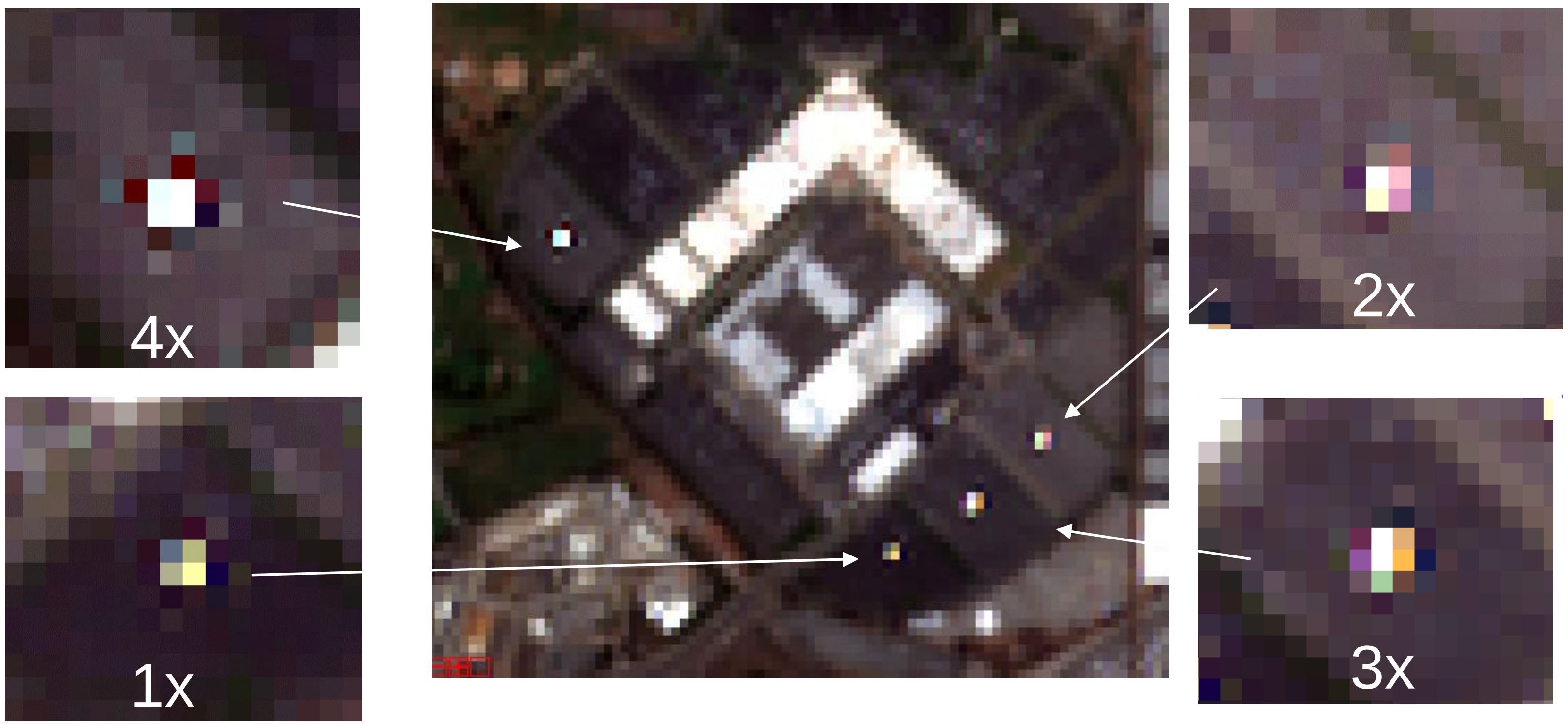

- Resampling methods need to be improved so as to use the PSF/MTF information to direct the energy back into the pixel that contains the target.

Sentinel 2 Band 3 Images of SPARC Targets

Four targets set up in Raytheon El Segundo campus parking lot to providing a uniform background.

Targets set up to produce four quantized upwelling intensities made from 1, 2 ,3 and 4 identical mirrors designed to produce responses across the sensor dynamic range.

July 8, 2016

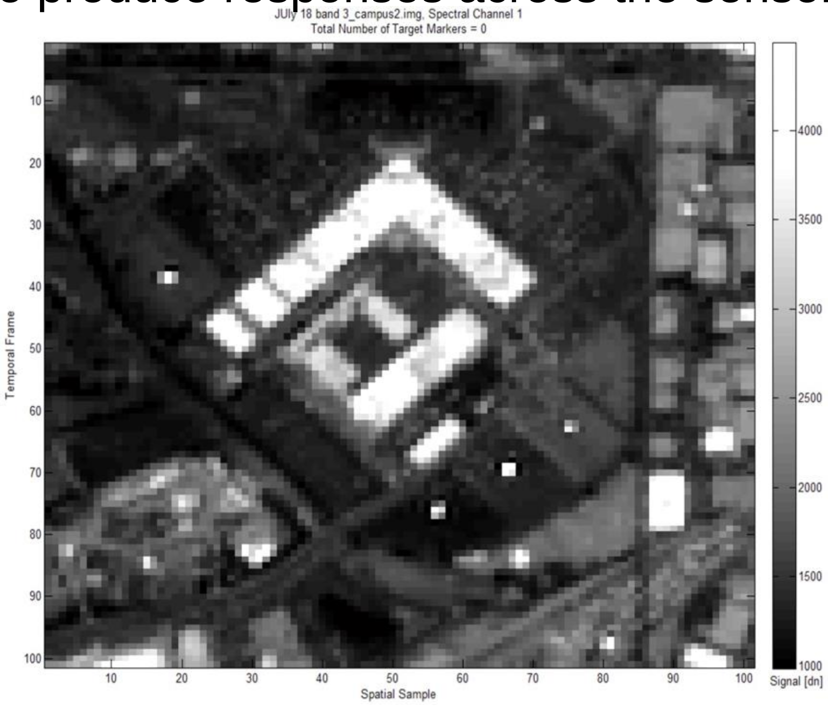

July 18, 2016

August 7, 2016

The three brightest from each image are used to generate an oversampled point spread function.

System PSF shows the effects on the SPARC targets from producing a georeferenced resampled product

10 m GSD Green Band Images (Band 2)

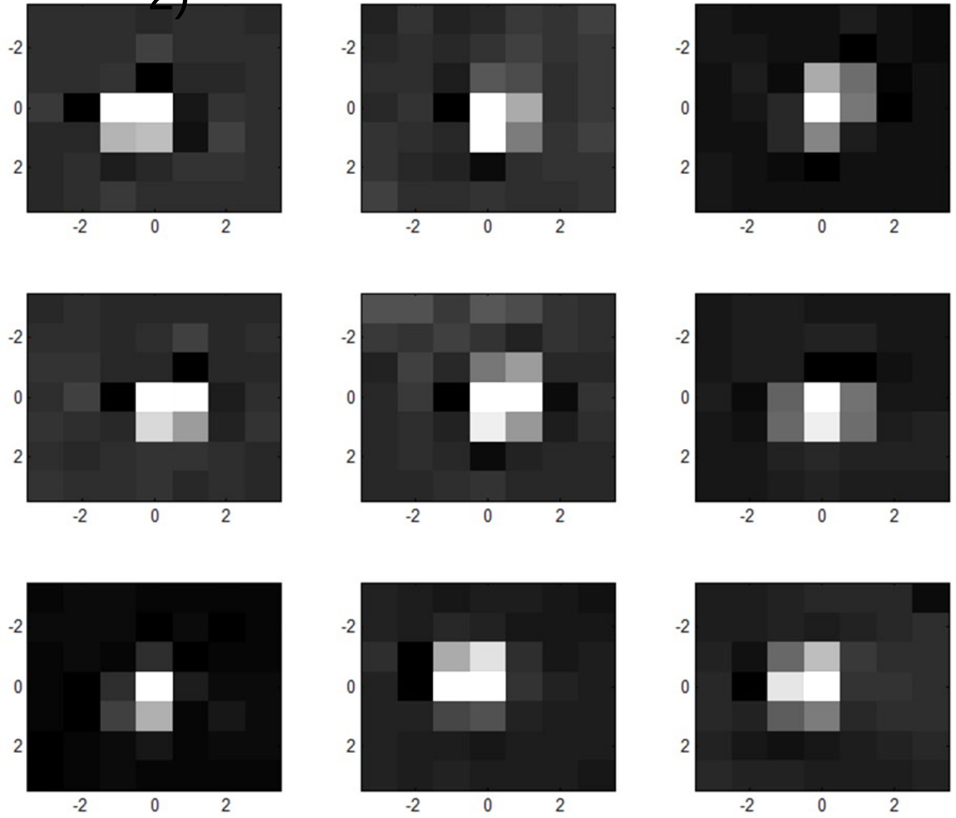

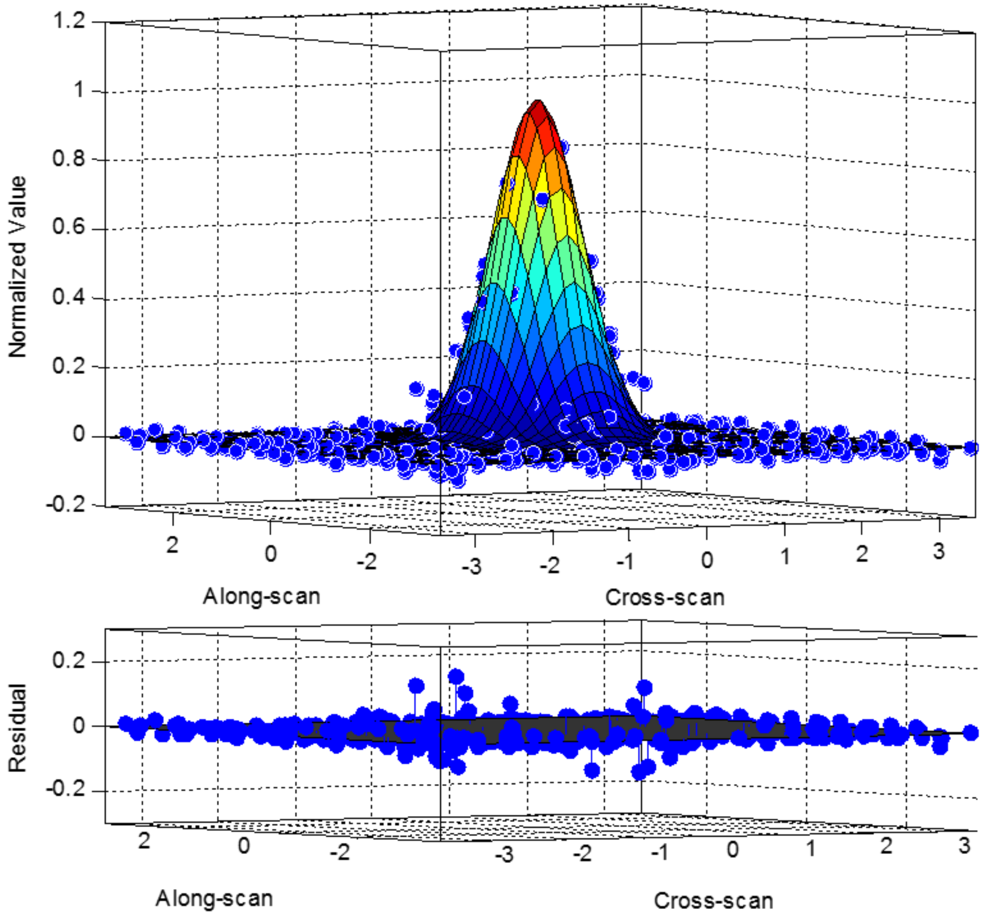

>1 m diameter SPARC targets visibly impacts a 5x5 pixels area

Sentinel 2 Cross-Scan and Along-Scan Profile

Green Band

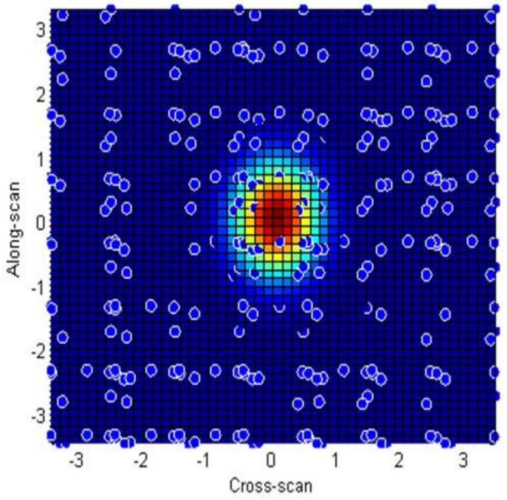

Green Band Semi-Parametric Pr

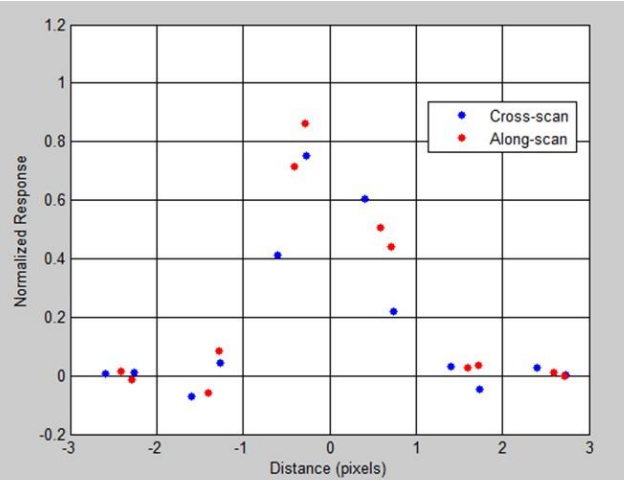

NIR Band

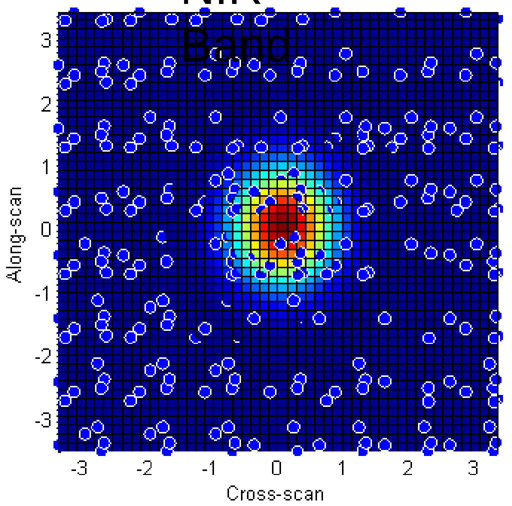

NIR Band Semi-Parametric Profile

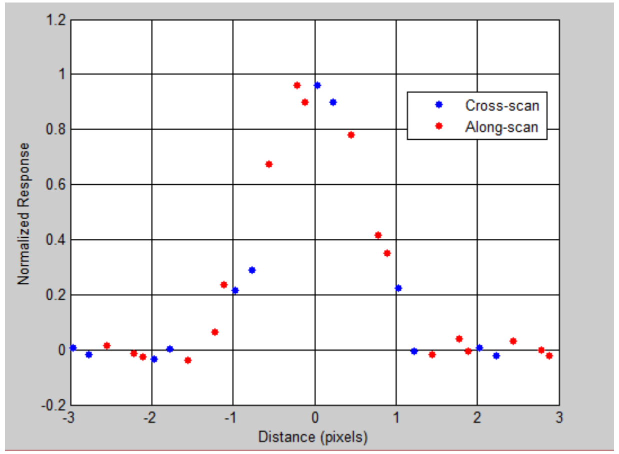

Gaussian Model PSF FWHM

10 m GSD Spectral Band	Cross-Scan PSF FWHM (Pixels)	Along Scan PSF FWHM (Pixels)
Blue	1.15	1.20
Green	1.06	1.40
Red	1.22	1.42
NIR	1.25	1.48

Linear Response To Target Integrated Radiance

Green band image (Band 3)

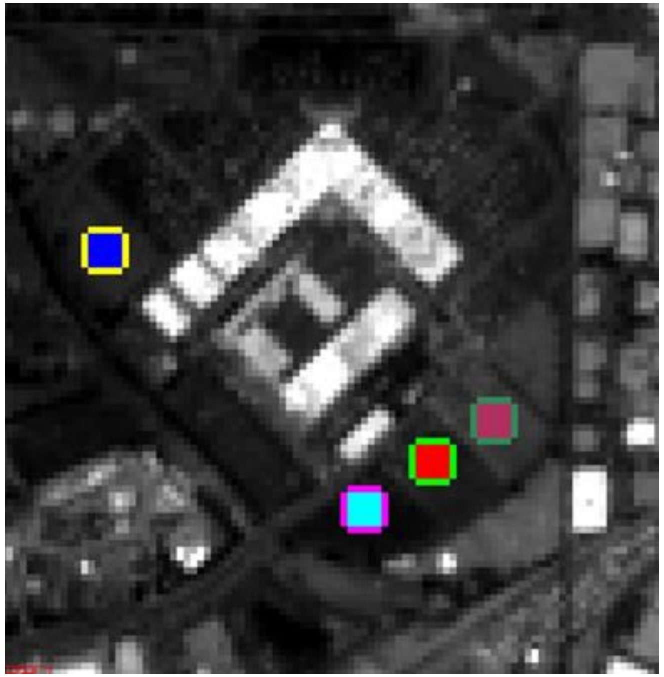

Target Integration windows and background sampling for background subtraction

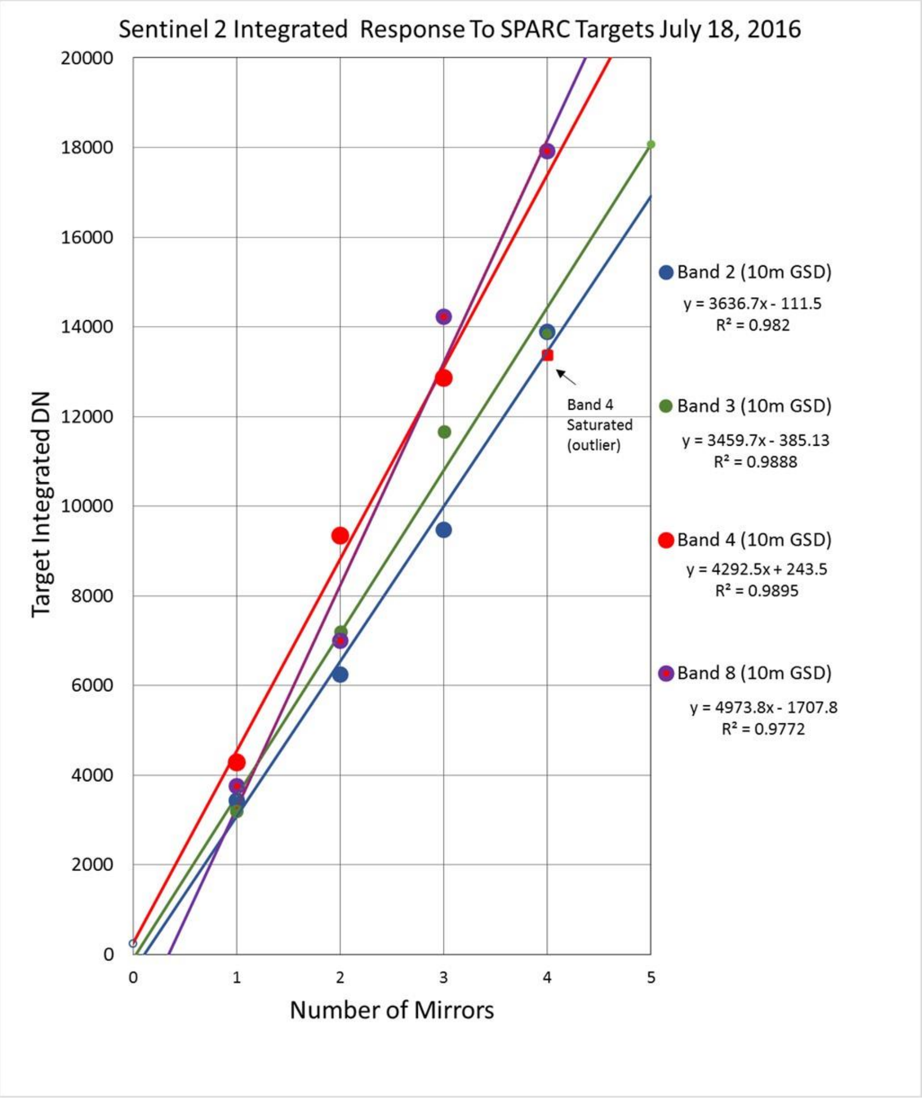

Summary

- The application of the SPARC vicarious calibration method, initially demonstrated to achieve >3% absolute calibration for high spatial resolution sensors, has been demonstrated to be scalable to moderate resolution system.
- Lessons learned from initial performance assessment with Landsat and Sentinel 2 will be applied with the expectation to achieve similar absolute calibration performance with moderate resolution sensors
- Important because this is the only vicarious calibration method that can directly address small target radiometry issues
- Target design was successful at maintaining a compact system and ease of deployment
- Targets can potentially be applied to sensor systems with a GSD out to 100 m
- Potential to be developed as a permanent calibration site and provide RadCalNet capabilities for radiometric, image quality and geometric performance assessment.